Optically detected magnetic resonance studies of point defects in Ga(Al)NAs

I. P. Vorona,* T. Mchedlidze, D. Dagnelund, I. A. Buyanova, and W. M. Chen†
Department of Physics and Measurement Technology, Linköping University, 58183 Linköping, Sweden

K. Köhler
Fraunhofer-Institut für Angewandte Festkörperphysik, Tullastrasse 72, D-79108 Freiburg, Germany
(Received 13 December 2005; revised manuscript received 8 March 2006; published 30 March 2006)

An optically detected magnetic resonance (ODMR) study of Ga(Al)NAs alloys grown by molecular beam epitaxy on GaAs substrates is presented. A number of grown-in defects were observed which act as nonradiative recombination centers. A detailed analysis of experimental data using a spin Hamiltonian leads to the identification of two Ga_i defects. A comparison with similar defects in other phosphide-based diluted nitride *III-V* compounds, such as GaAlNP and GaInNP, allows us to obtain additional information about the nearest surrounding of the defects. A discussion of possible models for other defects observed in the experiments is also presented.

DOI: 10.1103/PhysRevB.73.125204 PACS number(s): 76.70.Hb, 61.72.Ji, 71.55.Eq

I. INTRODUCTION

Point defects in various semiconductor materials are of strong interest both academically and technologically. Interstitials, vacancies, and antisites have been found to be commonly occurring defects in semiconductor crystals.[1,2] They can also form different defect complexes and participate in creation of extended defects. They have been shown to play an important role in determining electrical and optical properties of semiconductors and performance of related devices. In some particular cases, defects can help in controlling certain properties of materials, for example, management of carrier lifetime and Fermi level position by introducing antisite related defects in GaAs (Refs. 3 and 4) and InP (Refs. 5 and 6). Unfortunately, in most cases, they lead to degradation of properties essential for device operations. Therefore, knowledge about nature and formation mechanisms of defects and their influence on physical properties of semiconductor materials is necessary in order to control them. In the case of diluted nitrides, the issue of defects has become very important because required nonequilibrium growth provides favorable conditions for defect formation. Unfortunately, chemical identification of point defects in Ga(In)NAs alloys has so far been experimentally verified only in a few cases, which are related to N interstitials, Ga vacancies, and As_{Ga} antisites.[7–13] To our knowledge, chemical identification of point defects in GaAlNAs has not been reported so far in the literature.

Recently, it has been shown that Ga interstitials are the dominant grown-in defects in phosphide-based dilute nitrides, namely Ga(Al)NP alloys.[14]The aim of the present work is to study and identify important grown-in defects in arsenide-based dilute nitride Ga(Al)NAs and to obtain information about their role in carrier recombination processes.

II. EXPERIMENTAL DETAILS

Quaternary Ga(Al)NAs samples used for this study were grown on (100) GaAs substrates in a Varian Gen II Modular molecular-beam epitaxy (MBE) system using Al, Ga, and As solid sources and an rf nitrogen plasma source without a deflection plate. The growth rate was about 1.25 μm/h. The growth temperature was in the range of 570 °C to 580 °C. The typical thickness of the alloys was 0.1 μm. The Al content of investigated samples varied from 0 to 5%. Two sets of alloys were studied, one with a nitrogen content of 0% and the other of 1%.

Most of optically detected magnetic resonance (ODMR) measurements were performed with a modified Bruker ER 200 D *X* band (~9.3 GHz) with a liquid helium flow cryostat. The 532 nm line of a solid-state laser was used as an excitation source. An ODMR signal was detected using a lock-in technique as a change of photoluminescence (PL) intensity due to on-off modulation of microwave power as a function of magnetic field, by monitoring the near-infrared spectral region by a cooled Ge detector. Complementary *W*-band (~95 GHz) ODMR measurements were carried out with an Oxford superconducting split-coil magnet (0–5 T) cryostat. Typical microwave power employed was 170–200 mW. The measurements were performed at 5 K.

III. RESULTS

Upon the above band-gap optical excitation, all Ga(Al)NAs alloys studied in this work exhibit PL emissions in the near-infrared spectral range (see the left panel of Fig. 1). Incorporation of Al in the alloys results in a strong decrease in intensity of the near-band-gap emission (near 1000 nm) that arises from band tail states, indicated by an arrow in Fig. 1. On the other hand, the longer-wavelength PL band related to deep-level defects (peaking at about $\lambda = 1500$ nm) does not change significantly if Al content does not exceed 3%. A further increase of the Al composition leads to a drastic decrease of both PL bands. Such decrease is often caused by introduction of defect-related nonradiative recombination centers during growth. In order to study and identify these defects, ODMR measurements were carried out. Representative ODMR spectra are shown in the right panel of Fig. 1, as a function of Al compositions. They were

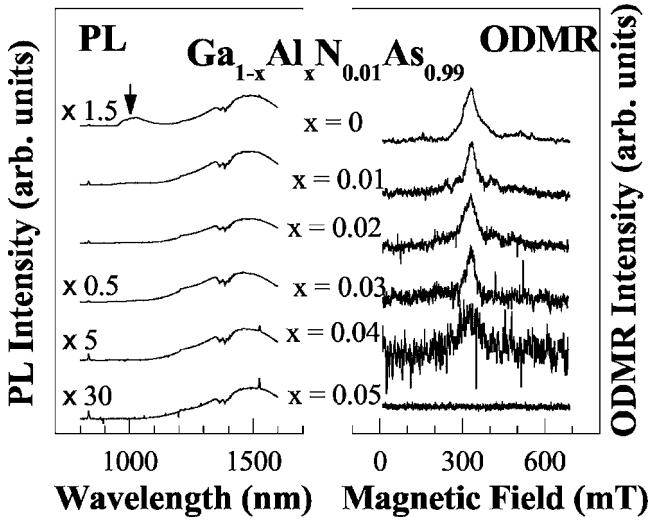

FIG. 1. Representative normalized PL and ODMR spectra from the Ga(Al)NAs samples studied in this work. The ODMR spectra were measured by monitoring all PL emissions over the spectral range of 900–1600 nm shown in the left panel. The sign of the ODMR signals is negative in all samples. They are shown as positive for easy viewing.

only observed in the nitrogen-containing alloys. A negative sign of the ODMR signals signifies that the corresponding defects act as nonradiative recombination centers, competing with the PL processes monitored via the entire spectral range shown on the left panel of Fig. 1.[15] The ODMR signals are shown as positive in Fig. 1 for easy viewing. In the Ga(Al-)NAs alloy with 5% of Al, however, ODMR signals were below the detection limit due to at least in part low intensity of the monitored PL.

A close examination of the ODMR spectra from the Ga(Al)NAs alloys revealed a complicated structure that consists of at least two components originating from different defects (Fig. 2). The first one is a strong line situated in the middle of the ODMR spectra with a g value close to 2 (denoted as the "middle line" below). This line is dominant in the ODMR spectra from the GaNAs alloy; whereas in GaAlNAs, its intensity becomes comparable with the second component of the ODMR spectra. The latter consists of a complicated pattern of lines spreading over a wide field range. In the spectrum from GaNAs, this component revealed well-resolved double lines at high fields and a few low-intensity lines at low fields [see Fig. 2(a)]. For the GaAlNAs alloys, these lines become broadened and shifted while additional lines appear. This finding shows that the second ODMR component contains at least two ODMR signals originating from different defects (denoted as Ga_i-A and Ga_i-B for the reason given below).

The multiline structure revealed in the second ODMR component can arise either from a high-electron spin state exhibiting a zero-field splitting caused by a defect crystal field or from a hyperfine (HF) interaction involving a high nuclear spin. A high-electron spin state with a zero-field splitting is known to produce strongly anisotropic ODMR spectra, whereas a HF interaction can lead to both isotropic and anisotropic ones. To clarify this issue, an angular depen-

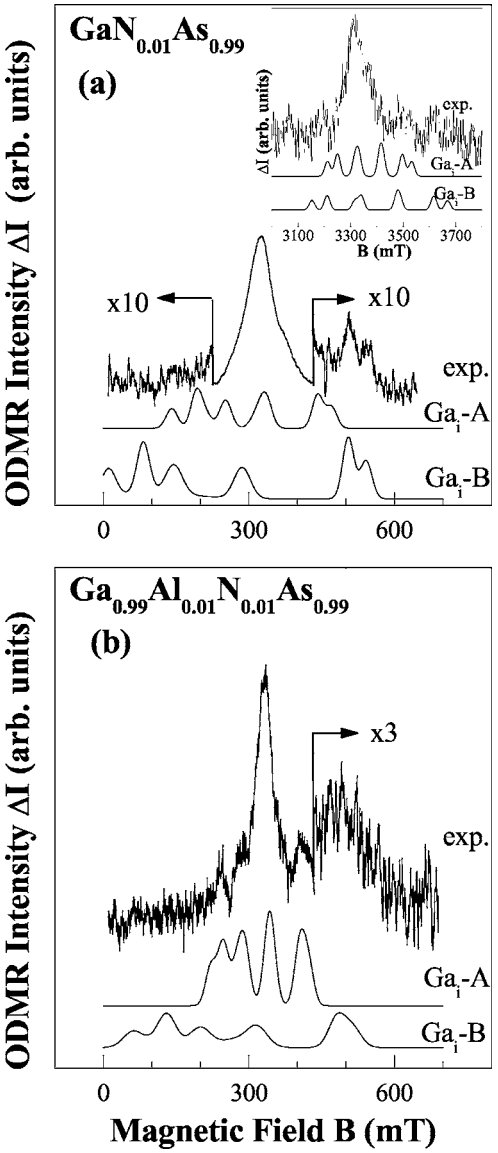

FIG. 2. Experimental ODMR spectra from the $GaN_{0.01}As_{0.99}$ (a) and $Ga_{0.99}Al_{0.01}N_{0.01}As_{0.99}$ (b), taken at 5 K at X band (9.31 GHz), and simulated spectra for the Ga_i-A and Ga_i-B complexes by using the spin Hamiltonian parameters given in Table I. An experimental ODMR spectrum from the $GaN_{0.01}As_{0.99}$ taken at W-band (95 GHz) is shown in the insert of (a), together with simulated spectra.

dence study was performed in a {110} crystallographic plane. Such measurements revealed that all lines attributed to the second ODMR component are isotropic, within the experimental accuracy. Thus, the ODMR spectra can be attributed to paramagnetic centers with effective electron spin $S=1/2$ involving high nuclear spins.

The doublet structure of the outer wings of the second ODMR component (Fig. 2) is characteristic for a HF interaction with an atom having two naturally abundant isotopes with nonzero magnetic moments. Only Ga satisfies this condition among all host atoms of the GaAlNAs alloys and possible contaminants. Thus, a Ga atom should be involved in the structure of the defects responsible for the ODMR spectrum. Since gallium has two isotopes (^{69}Ga and ^{71}Ga) with

TABLE I. Spin Hamiltonian parameters determined by fitting the spin Hamiltonian Eq. (1) to the experimental data for the Ga_i-*A* and Ga_i-*B* defects in $Ga_{1-x}Al_xN_{0.01}As_{0.99}$ samples studied.

x	0		0.01		0.02		0.03	
Defect	Ga_i-*A*[a]	Ga_i-*B*	Ga_i-*A*	Ga_i-*B*	Ga_i-*A*	Ga_i-*B*	Ga_i-*A*	Ga_i-*B*
S	1/2	1/2	1/2	1/2	1/2	1/2	1/2	1/2
I	3/2	3/2	3/2	3/2	3/2	3/2	3/2	3/2
g	2.005	1.98	2.003	1.98	2.003	1.98	2.003	1.98
$A(^{69}Ga)\times10^{-4}$ cm^{-1}	770	1250	490	1050	490	1050	490	1050
$A(^{71}Ga)\times10^{-4}$ cm^{-1}	1000	1590	620	1330	620	1330	620	1330

[a]Parameters are determined from the *W*-band ODMR measurements. At *X* band, the corresponding ODMR spectrum is masked by the more intensive middle line.

the same nuclear spin $I=3/2$, the ODMR spectra from the Ga-related defects should contain two quadruplets. The intensity ratio between the two quadruplets should be near 40/60 according to the natural abundance of these isotopes. The ratio of their line spacing should be near 1.3 in accordance with the ratio of nuclear magnetic moments between the two isotopes.

To confirm this hypothesis and obtain information on physical properties of the defects, a detailed analysis of the experimental data was performed by using an effective spin Hamiltonian

$$H = \mu_B \mathbf{B}\cdot\mathbf{g}\cdot\mathbf{S} + \mathbf{S}\cdot\mathbf{A}\cdot\mathbf{I}. \quad (1)$$

Here the first and second terms describe electron Zeeman and central HF interaction terms, respectively; μ_B is the Bohr magneton, **B** is the magnetic field, **g** is the Zeeman splitting tensor, and **A** is the central HF interaction tensor for each isotope. The effective electron spin is $S=1/2$ and the nuclear spin is $I=3/2$. By fitting the spin Hamiltonian to the experimental data, the spin Hamiltonian parameters were determined for both Ga_i-*A* and Ga_i-*B* in all samples and are shown in Table I. Both **g** and **A** tensors are deduced to be isotropic, within the experimental accuracy, and are reduced to the scalars *g* and *A*. Taken as an example, the simulated ODMR curves for the $GaN_{0.01}As_{0.99}$ and $Ga_{0.99}Al_{0.01}N_{0.01}As_{0.99}$ alloys are shown in Fig. 2, by using the spin Hamiltonian parameters in Table I and assuming a Gaussian line shape for each ODMR transition. The simulated spectra do agree with the experimental data that justifies the proposed model. The weaker intensity of the experimental ODMR lines at low fields as compared to that of the simulated ones can be attributed to the fact that the simulations only take into account the probabilities of magnetic-dipole allowed electron spin resonance transitions, but not the difference in recombination rates of the spin sublevels.[16,17] It can be concluded that the Ga_i-*B* defect is present in all N-containing Ga(Al)NAs alloys, even in the Al-free GaNAs, but Ga_i-*A* can only be clearly observed in GaAlNAs. (Note that a strong overlap with the more intensive middle line could mask the Ga_i-*A* ODMR spectrum in the Al-free GaNAs). Based on a striking similarity with the Ga_i-*A* and Ga_i-*B* defects observed in phosphide-based dilute nitride Ga(Al)NP reported earlier,[14] we strongly believe that the defects under study here are in fact the same Ga_i complexes but in two different dilute nitrides.

The strong middle line in the ODMR spectra from GaNAs revealed additional features that were observed more clearly on the high-field shoulder. This finding implies the presence of an additional substructure of the middle line. A similar substructure might also be present in the ODMR spectra from the GaAlNAs alloys but could be masked by the signals from the Ga_i complexes presented above. In order to obtain information on the substructure, we subtracted the simulated ODMR spectra of the Ga_i-*A* and Ga_i-*B* complexes from the experimental ones for the Al-containing GaAlNAs. The resulting spectra of the middle line are shown in Fig. 3 for three samples, clearly displaying a similar line shape consisting of several lines. Such a line shape can be described as a superposition of several lines in various ways. Some possible models for this substructure are presented in Fig. 4. Model 1 implies that it contains three independent single ODMR lines with different *g* values originating from three different paramagnetic defects. Another possibility is a superposition of a single line and a group of lines originating from an unresolved HF structure. The simplest HF line shapes resulting from an isotropic HF interaction with one nucleus of $I=3/2$ (gallium or arsenic) and of $I=1$ (nitrogen) are presented in Fig. 4 as model 2 and model 3, respectively.

The simplest distinction between model 1 and the other two models can be made by performing ODMR measure-

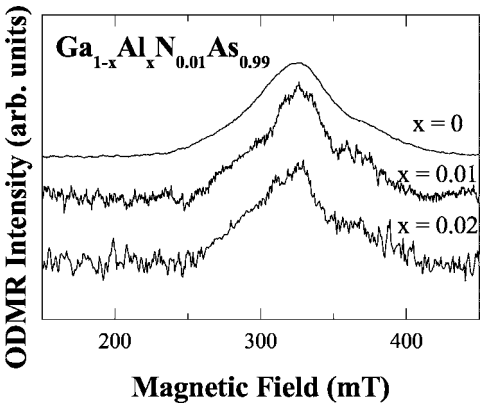

FIG. 3. A close-up of the middle line ODMR signal from the Ga(Al)NAs alloys, after subtracting the simulated Ga_i-*A* and Ga_i-*B* ODMR spectra from the experimental ones.

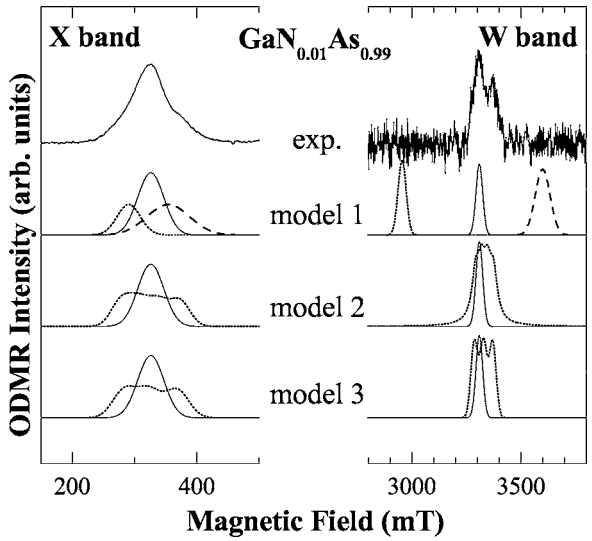

FIG. 4. Experimental and simulated ODMR spectra from $GaN_{0.01}As_{0.99}$ at both *X*-band (9.31 GHz) and *W*-band (94.8 GHz). The simulated ones include the contributions from three single lines in model 1, a superposition of a single line (solid) and an unresolved HF quadruplet (dotted) in model 2, and a superposition of a single line (solid) and an unresolved HF triplet (dotted) in model 3.

ments at two different microwave frequencies. This is because the field separation between different ODMR lines with different g values in model 1 should scale with the microwave frequency. On the contrary, the line spacing caused by a HF interaction as proposed by models 2 and 3 will be nearly independent of the microwave frequency used. Figure 4 presents both *X*-band and *W*-band ODMR spectra from the GaNAs alloy. It is clearly seen that the middle line has a similar linewidth at both microwave frequencies, thus concluding that the substructure must be due to an unresolved HF structure. A slight modification of the line shape between the ODMR spectra at the two microwave frequencies could be caused by a slightly different contribution in intensity from the single line that overlaps with the unresolved HF structure discussed above.

IV. DISCUSSION

From the previous study in Ga(Al)NP, it was assumed that Ga_i-*A* is probably located in the T_d-symmetry interstitial position surrounded by group-III atoms.[14] The present data seems to confirm this assumption. The strengths of the HF interaction of Ga_i-*A* in the Al-containing GaAlNAs determined in this study are equal to 490×10^{-4} cm^{-1} and 620×10^{-4} cm^{-1} for ^{69}Ga and ^{71}Ga, respectively. These values are very close to that in AlGaNP [$A(^{69}\text{Ga})=(450-490)\times10^{-4}$ cm^{-1}] (Ref. 14) and in (Al,Ga)As-based structures [$A(^{69}\text{Ga})=(480-540)\times10^{-4}$ cm^{-1}] (Refs. 18–21). Assuming that a similar Ga_i defect complex is involved, the similarity in the HF strengths seems to suggest that the defect has the same nearest surrounding in these systems. This is possible only when the Ga_i occupies an interstitial position with group-III atoms in the nearest environment. Moreover, similar to GaAlNP, the HF interaction strength in GaAlNAs decreases with incorporation of Al. For example, the value of $A(^{69}\text{Ga})$ decreases from 770×10^{-4} cm^{-1} for GaNAs (this study) and GaNP (Ref. 14) to 490×10^{-4} cm^{-1} for GaAlNAs (this work) and $(450-490)\times10^{-4}$ cm^{-1} for GaAlNP (Ref. 14). Apparently this should indicate a direct involvement of aluminum atom(s) in the nearest surrounding of defects in the Al-containing alloys. In GaAlNP, this was attributed to a possible site exchange between a substitutional Ga atom and an interstitial Al atom due to a stronger bonding between Al and the group-V atoms, resulting in an interstitial Ga atom and a substitutional Al (Ref. 14). A similar mechanism can also possibly be responsible for the present case of GaAlNAs. This attribution seems to be consistent with the earlier experimental finding of preferred Al-N bonding (Refs. 22 and 23). Note that the strength of the HF interaction of Ga_i-*A* in GaNAs and GaNP, $A(^{69}\text{Ga})=770\times10^{-4}$ cm^{-1}, is very close to 741×10^{-4} cm^{-1} observed for the Ga_i in GaP (Ref. 24) that may be considered as another piece of evidence for the similarity in the nearest surroundings of the defect.

On the other hand, the Ga_i-*B* defect was never observed in nitrogen-free GaP and GaAs alloys. This may indicate that either the N atom could be directly involved in the structure of the Ga_i-*B* defect or the growth conditions required for the incorporation of N strongly facilitate the defect formation. The HF strength $A(^{69}\text{Ga})$ of Ga_i-*B* in GaNAs determined in this study is equal to 1250×10^{-4} cm^{-1}. This value slightly differs from the value of 1150×10^{-4} cm^{-1} in GaNP (Ref. 14). This may indicate a difference in the nearest surrounding of the defect between these two alloys that should be related to the group-V atoms. In a tetrahedral semiconductor like GaNAs or GaAlNAs there are two different interstitial positions with group-V atoms in the nearest surrounding. These are the T_d-symmetry position surrounded only by group-V atoms and the D_{3v}-symmetry position with both group-III and group-V atoms as the nearest neighbors. From the observed dependence of the HF strength on Al compositions, namely a decrease of the HF strength $A(^{69}\text{Ga})$ from 1250×10^{-4} cm^{-1} (Al-free) to 1050×10^{-4} cm^{-1} (Al-containing) in Ga(Al)NAs and from 1150×10^{-4} cm^{-1} (Al-free) to 980×10^{-4} cm^{-1} (Al-containing) in Ga(Al)NP, it is tempting to suggest that the Ga_i-*B* defect could reside in the D_{3v}-symmetry interstitial position.

Similar to the case of GaAlNP, both Ga_i-*A* and Ga_i-*B* are believed to be complexes involving a Ga_i, rather than the isolated Ga_i residing at two inequivalent interstitial sites.

Besides GaAlNP (Ref. 14), Ga interstitials complexes were also previously suggested to be present in GaInNP alloys (Ref. 25). Our present finding of Ga_i in Ga(Al)NAs alloys shows that they are common point defects in various diluted nitrides. Apparently, the specific character of growth processes required for diluted nitride alloys, such as low substrate temperatures, nitrogen incorporation, or associated ion bombardment, etc., have created favorable conditions for the formation of these defects.

In contrast to the Ga_i complexes, the origin of the middle line in the ODMR spectrum from the Ga(Al)NAs alloys cannot unfortunately be positively identified. The cross-examination by both *x*-band and *w*-band ODMR measure-

ments (Fig. 4) clearly shows that the broad linewidth (full width more than 100 mT) is caused by an unresolved HF structure. A possible source of the HF interaction can arise from the host atoms with nonzero nuclear spins, i.e., $I=1$ (N) and $I=3/2$ (Ga and As) in GaNAs (see Fig. 4). Assuming only one nucleus is involved, the values of the HF parameter A estimated from the linewidth are $\sim 260\times 10^{-4}$ cm^{-1} and $\sim 400\times 10^{-4}$ cm^{-1} for $I=3/2$ and $I=1$, respectively. These host atoms, if they are the nearest neighbors of the defect, can also be the source of ligand HF structure. Unfortunately, a lack of resolved HF structure of the middle line does not allow us to determine the exact number and values of the nuclear spins involved, which would otherwise shed light on the chemical identity of the responsible defect.

It is interesting to note that the As_{Ga} antisites defect, previously found to be predominant in Ga(In)NAs grown at low temperatures (e.g., at 420 °C) by gas-source MBE (Refs. 11–13), was not observed in the Ga(Al)NAs alloys studied in this work. We believe that the higher growth temperature of 570 °C to 580 °C used for the latter is the major factor that has strongly suppressed the formation of the As_{Ga} antisites defect, consistent with the previous study.[11–13]

The negative sign of the ODMR signals for all studied defects represents a decrease in the intensity of the PL emissions over the monitored spectral range of 900–1600 nm upon spin resonance transitions. The fact that the ODMR signals from the four different defects studied here can be detected via the same two PL bands (shown in the left panel of Fig. 1) provides strong evidence that the defects are not directly involved in the radiative recombination processes giving rise to the PL. Instead, they are nonradiative recombination centers that compete with the monitored radiative recombination processes. Due to this competition, increasing carrier recombination via these nonradiative centers induced by the spin resonance transitions will consequently lead to the observed decrease in the monitored PL intensity. The observation that the introduction of the two Ga_i-related defects promoted by the incorporation of N and Al in the alloys is accompanied by a decrease in the intensity of the monitored PL emissions, especially for the one near the band edge, supports the conclusion that the defects play an important role in degrading the optical quality of the alloys.

V. CONCLUSIONS

In conclusion, we have studied and identified two different Ga_i defects in Ga(Al)NAs alloys, namely Ga_i-*A* and Ga_i-*B*. The involvement of a Ga_i in both defects is concluded from its unique HF interaction and similarity to Ga(Al)NP studied previously. This finding shows that Ga interstitials are common intrinsic defects in various diluted nitrides. The obtained results seem to support that Ga_i-*A* is surrounded by group-III atoms while Ga_i-*B* has both group-III and group-V atoms in the nearest neighborhood. The middle line ODMR signals observed at around $g=2$ are suggested to arise from superposition of a defect with a single ODMR line and a defect with an unresolved HF structure. All defects studied are shown to act as nonradiative recombination centers, competing with the radiative recombination processes monitored in ODMR, and are therefore harmful for device performance if the alloys are to be utilized as active regions of light-emitting devices.

ACKNOWLEDGMENTS

The financial support by the Swedish Research Council and the Wenner-Gren Foundation is greatly appreciated.

*Permanent address: Institute of Semiconductor Physics, Pr. Nauky 45, Kiev 03028, Ukraine.

†Corresponding author. Electronic mail: wmc@ifm.liu.se

[1] G. F. Neumark, Mater. Sci. Eng., R. **21**, 1 (1997).

[2] F. K. Koschnick and J.-M. Spaeth, Phys. Status Solidi B **216**, 817 (1999).

[3] G. M. Martin and S. Makram-Ebeid, in *Deep Centers in Semiconductors*, edited by S. Pantelides (Gordon and Breach, New York, 1986), p. 389.

[4] X. Liu, A. Prasad, W. M. Chen, A. Kurpiewski, A. Stoschek, Z. Liliental-Weber, and E. R. Weber, Appl. Phys. Lett. **65**, 3002 (1994).

[5] W. M. Chen, I. A. Buyanova, A. V. Buyanov, T. Lundström, W. G. Bi, and C. W. Tu, Phys. Rev. Lett. **77**, 2734 (1996).

[6] W. M. Chen, P. Dreszer, A. Prasad, A. Kurpiewski, W. Walukiewicz, E. R. Weber, E. Sörman, B. Monemar, B. W. Liang, and C. W. Tu, J. Appl. Phys. **76**, 600 (1994).

[7] S. G. Spruytte, C. W. Colden, J. S. Harris, W. Wampler, P. Krispin, K. Ploog, and M. C. Larson, J. Appl. Phys. **89**, 4401 (2001).

[8] W. Li, M. Pessa, T. Ahlgren, and J. Decker, Appl. Phys. Lett. **79**, 1094 (2001).

[9] T. Ahlgren, E. Vainonen-Ahlgren, J. Likonen, W. Li, and M. Pessa, Appl. Phys. Lett. **80**, 2314 (2002).

[10] J. Toivonen, T. Hakkarainen, M. Sopanen, H. Lipsanen, J. Oila, and K. Saarinen, Appl. Phys. Lett. **82**, 40 (2003).

[11] N. Q. Thinh, I. A. Buyanova, P. N. Hai, W. M. Chen, H. P. Xin, and C. W. Tu, Phys. Rev. B **63**, 033203 (2001).

[12] N. Q. Thinh, I. A. Buyanova, W. M. Chen, H. P. Xin, and C. W. Tu, Appl. Phys. Lett. **79**, 3089 (2001).

[13] W. M. Chen, N. Q. Thinh, I. A. Buyanova, H. P. Xin, and C. W. Tu, in *Progress in Semiconductor Materials for Optoelectronic Applications*, edited by Eric D. Jones, Omar Manasreh, Kent D. Choquette, Daniel J. Friedman, and Daniel K. Johnstone, MRS Symposia Proceedings No. 692 (Materials Research Society, Pittsburgh, 2002), 67.

[14] N. Q. Thinh, I. P. Vorona, I. A. Buyanova, W. M. Chen, Sukit Limpijumnong, S. B. Zhang, Y. G. Hong, H. P. Xin, C. W. Tu, A. Utsumi, Y. Furukawa, S. Moon, A. Wakahara, and H. Yonezu, Phys. Rev. B **71**, 125209 (2005).

[15] W. M. Chen, and B. Monemar, Appl. Phys. A: Solids Surf. **A53**, 130 (1991).

[16] W. M. Chen, Thin Solid Films **364**, 45 (2000).

[17] W. M. Chen, in *EPR of Free Radicals in Solids*, edited by A.

Lund and M. Shiotani (Kluwer Academic Pub., Dordrecht, 2003), p. 601.
[18] T. A. Kennedy and M. G. Spencer, Phys. Rev. Lett. **57**, 2690 (1986).
[19] T. A. Kennedy, R. Magno, and M. G. Spencer, Phys. Rev. B **37**, 6325 (1981).
[20] J. M. Trombetta, T. A. Kennedy, W. Tseng, and D. Gammon, Phys. Rev. B **43**, R2458 (1991).
[21] T. Wimbauer, M. S. Brandt, M. W. Bayerl, N. M. Reinacher, M. Stutzmann, D. M. Hofmann, Y. Mochizuki, and M. Mizuta, Phys. Rev. B **58**, 4892 (1998).
[22] T. Geppert, J. Wagner, K. Köhler, P. Ganser, and M. Maier, Appl. Phys. Lett. **80**, 2081 (2002).
[23] J. Wagner, T. Geppert, K. Köhler, P. Ganser, and M. Maier, Appl. Phys. Lett. **83**, 2799 (2003).
[24] K. M. Lee, in *Defects in Electronic Materials*, edited by M. Stavola *et al.*, MRS Symposia Proceedings No. 104 (Material Research Society, Pittsburgh, 1988), p. 449.
[25] I. P. Vorona *et al.*, Appl. Phys. Lett. **86**, 222110 (2005).